Optical and Hot-Film Measurements of the Boundary Layer Transition on a Naca Airfoil

David Šimurda[1], *Jindřich* Hála[1], *Martin* Luxa[1], and *Tomáš* Radnic[1]

[1]Institute of Thermomechanics of the Czech Academy of Sciences, Dolejskova 1402/5, 18200, Prague, Czech Republic

Abstract. This study explores the possibilities of identifying position of a boundary layer transition using hot film measurements complemented by classical optical methods i.e. interferometry and schlieren method. The subject of the measurement is a NACA 0010-64 airfoil with varying leading edge surface quality corresponding to smooth surface and rough surface with Ra ~ 50 and Ra ~ 100. Measurements are performed at several subsonic regimes and a transonic regime. Despite several shortcomings of the experimental setup, the method proved to be useful in providing information on the boundary layer transition. Measurements show that in the case of smooth leading edge, the onset of the boundary layer transition shifts upstream with increasing inlet Mach number and the major portion of the boundary layer is transitional. This is in accordance with other published results on the boundary layer transition on this kind of airfoils [1]. In all cases with the rough leading edge, the complete transition takes place on the rough portion of the surface already.

1 Introduction

Development of a boundary layer on blade surfaces and its transition from laminar to turbulent is an important aspect of the design of turbomachinery bladings. It is important mainly in transonic and supersonic regimes of operation when a boundary layer interacts with a shock wave. In such cases, the turbulent boundary layer is preferable at the point of interaction as it can withstand larger pressure gradients than the laminar boundary layer. This plays role namely in the case of rotor blade tip sections of transonic compressors and the last rotor tip sections of large steam turbines. The latter operate at supersonic regimes and the interaction of the inlet shock wave with the pressure side boundary layer takes place in the relatively short and narrow interblade channel, thus having significant impact on the main flow. [2]

Additionally, real shape and surface quality of a real blade profile may be significantly different from the nominal design due to manufacture or erosion. Therefore, possible changes in the shape and surface roughness should also be taken into account during the design. Yet, this may be a problem for CFD solvers which are nowadays vastly used in the design process. Transitional turbulence models do not always satisfactorily predict the boundary layer transition when an increased surface roughness is present. Thus, the existing transitional turbulence models need to be enhanced and their performance validated on a particular geometry of interest and at particular flow conditions. Therefore, introductory measurements of the boundary layer transition were done on an isolated NACA 0010-64 airfoil with the intention to measure the boundary layer transition on supersonic tip sections of large output steam turbines in the future. Experience with the measurement and its results are described in the paper.

2 Measured model

Optical and hot-film measurements were done on an isolated symmetric NACA 0010-64 airfoil. This particular airfoil was chosen as appropriate with respect to higher subsonic and up to transonic velocities taking place on the airfoil surface at investigated regimes. The model was fixed in the wind tunnel test section using two supporting steel stripes (Fig. 1). This way of fixing was necessary since side-walls of the wind tunnel test section had to be equipped with fine optical glass windows that did not allow fixing of the model straight to the sidewalls. Supporting stripes were shaped so that they obstructed field of vision as little as possible.

Upper surface of the airfoil was equipped with a custom *Senflex* hot-film array consisting of 16 sensing elements on a foil with an adhesive. The

* Corresponding author: simurda@it.cas.cz

foil was adhered to the airfoil according to Figure 2. Prior to the application of the hot-film foil, part of the model under the sensing elements was milled in the depth of 1 mm and filled with heat insulation putty to minimize heat flux from the films to the steel model. Leadwires connecting leads of sensing elements with the measuring system were covered with resin and sanded smooth to the airfoil surface. (Fig. 3)

Fig. 1. Model of airfoil with supporting stripes

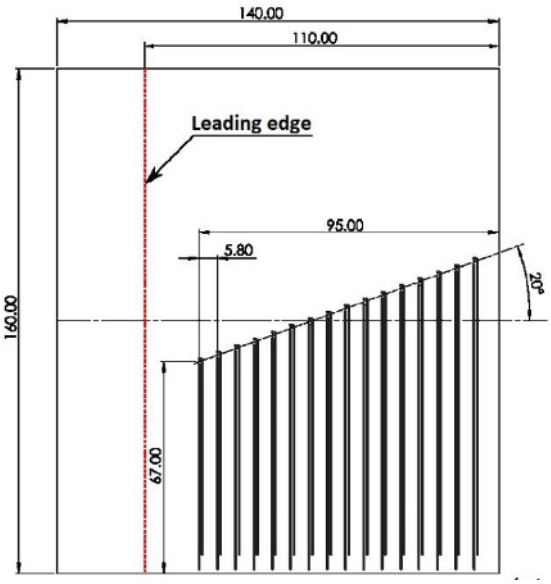

Fig. 2. Shape of the foil with array of hot-films that was adhered to the upper surface of the airfoil

Different values of leading edge roughness were realized by a double sided tape of 0.08 mm thickness. When adhered to the airfoil, the upper side of the tape was covered with corundum grains of specific roughness. In this research, grains forming roughness Ra~50μm and Ra~100μm were used. Such values roughly represent surface of erosion-worn steam turbine blades . The rough tape covered front 25% of the airfoil chord (Fig. 4).

The model equipped with the hot-film array and rough leading edge is shown in Figure 5.

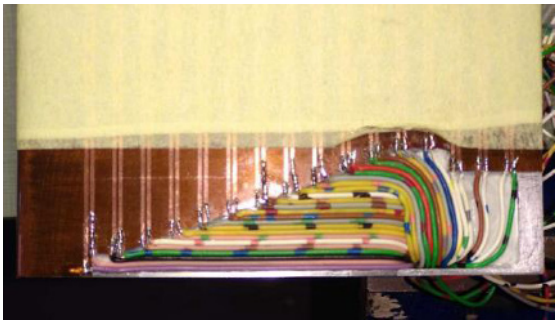

Fig. 3. Arrangement of soldered leadwires

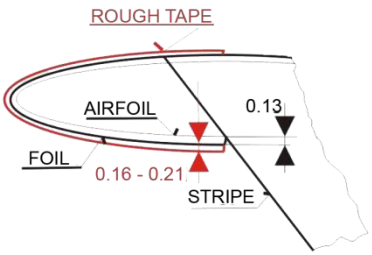

Fig. 4. Layer composition on the leading edge showing thicknesses and coverage of hot-film foil and rough tape

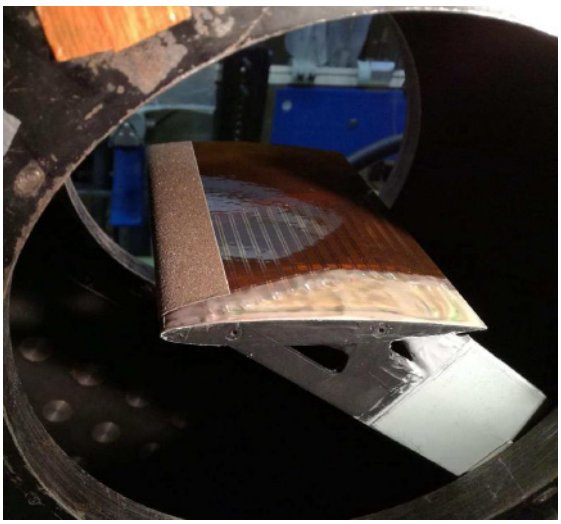

Fig. 5. The model with hot-film foil and rough tape mounted in the wind tunnel test section

3 Measurements

Measurements were done in the suction type high-speed wind tunnel of the Institute of Thermomechanics of the Czech Academy of Scinces in Nový Knín (Fig. 6).

Model in the test section was set at zero incidence position at all investigated regimes.

Flow parameters were measured by a Prandtl probe and static pressure tappings on the side-wall in front of the model. Static pressure was also measured by two tappings on the upper surface of the model and one tapping on the bottom surface of the model. These readings were utilized for evaluation of interferograms.

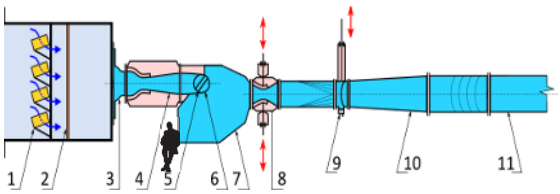

Fig. 6: Scheme of the intermittent suction type high-speed wind tunnel: 1–silica gel dryer, 2–filters, 3–entrance nozzle, 4–inlet nozzle, 5–transient insert, 6–turn-around test section, 7–settling chamber, 8–control nozzle, 9– quick acting valve, 10–diffuser, 11–main duct

Hot-Film measurements were done using the *A. A. LabSystems AN-1003* anemometric system operated in CTA mode. Sensing elements were held at constant temperature 110 °C. Based on the *square-wave/pulse test* [5], the sampling frequency was set to 50kHz with 16kHz low-pass filter. Samples were acquired by *National Instruments DAQ* card for 0.5s for each channel. Character of the boundary layer was evaluated from the acquired signal based on the signal skewness function SF:

$$SF = \frac{\frac{1}{m}\sum_0^m (v_b' - \bar{V}_b)^3}{\left(\frac{1}{m}\sum_0^m (v_b' - \bar{V}_b)^2\right)^{2/3}} \quad (1)$$

According to Hodson [3] and Tiedemann [4], SF is positive at the onset of the boundary layer transition and negative at its completion. Both laminar and fully turbulent boundary layers are characterized by zero value of SF.

Table 1. Regimes investigated by optical methods OM and/or hot-film measurements H-F

(● - measured, ■ - measured also by Schlieren technique)

M_1	Smooth LE		LE Ra~50		LE Ra~100	
	OM	H-F	OM	H-F	OM	H-F
0.3		●				
0.5		●		●		
0.75	●■	●	●■	●	●	●
0.97	●■	●	●■	●	●	●

It turned out that not all sensing elements were functioning; therefore, further analyses were done with signals from elements no. 2, 6, 8, 9, 11, 12, 14, 15, 16. In the case of rough leading edge, number of front elements was covered with the tape. Thus only the signal from elements no. 6, 8, 9, 11, 12, 14, 15 and 16 could be evaluated.

Optical measurements consisted of interferometry and Schlieren technique. Interferograms were obtained using Mach-Zehnder interferometer setup for infinite fringe method. Schlieren pictures were taken with optical setup in Toepler configuration.

Measured regimes are provided in Table 1.

4 Shortcomings and limits of adopted approach

4.1 Asymmetry

Despite the fact that the model is a symmetric airfoil and that it was set at zero incidence in the test section, design of the model and the way of fixing the hot-film foil cause certain asymmetry. Main reason is the use of supporting stripes which create an obstacle on the side-walls under the model. Hence, these stripes change the cross-sectional area of the flow channel under the model by 3.1% influencing the development of the side-wall boundary layers. Additionally, the foil with the hot-film array creates a backward facing step on the lower surface of the airfoil at 25% of the chord. Height of this step is about 0.13mm as can be seen in Figure 3.

Due to this asymmetry, real effective angle of attack is slightly negative. Based on the shape of interference fringes at the leading edge (Figs. 7, 8, 9), the shift towards negative values was estimated to be (2÷4)°. Interferograms in Figures 7, 8 and 9 document higher flow acceleration on the lower surface. This leads to an earlier origin of a supersonic region on the lower surface (Fig. 8) and thickening of the boundary layer there due to interaction with the normal shock terminating this region. At higher inlet Mach number when a supersonic region covers major portion of the airfoil (Fig. 9), the step due to foil with hot-film array results in an origin of the oblique shock. Nevertheless, the supersonic region is about the same size on both surfaces. On the lower surface, the boundary layer separation due to interaction with the normal shock wave terminating supersonic region is more pronounced.

4.2 Imperfect coverage of leadwires

Leadwires soldered to leads of sensing elements were covered with resin as can be seen in Figures 3 and 5. Span-wise size of the region with covered leadwires increases towards trailing edge. In the last 30% of the chord it covers approximately 19% of the span. However, the coverage surface is not perfectly smooth and it causes disturbances to the flow which are captured by the used optical

methods (Fig. 10). These disturbances, nevertheless, take place only at a region close to side-wall and they do not disturb flow at the midspan.

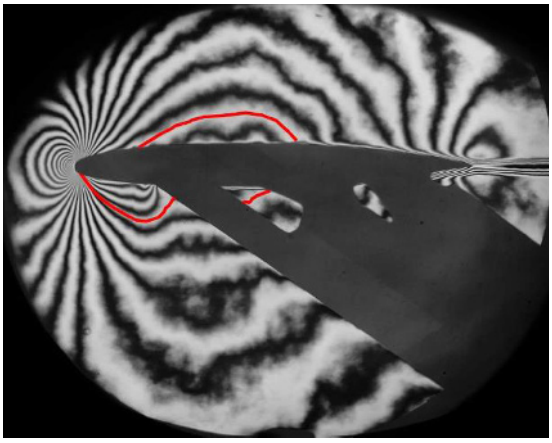

Fig. 7. Interferogram with highlighted fringe of constant velocity; taken at subsonic regime (M_1 = 0.752), smooth leading edge

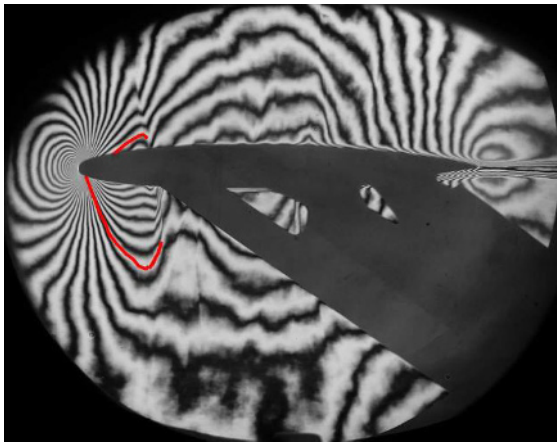

Fig. 8. Interferogram with highlighted fringe of constant velocity; taken at transonic regime (M_1 = 0.850), smooth leading edge

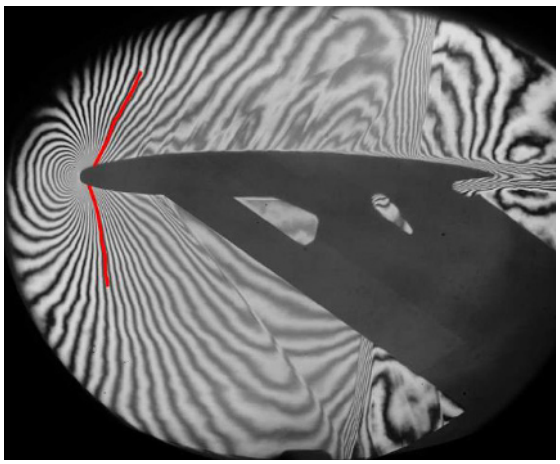

Fig. 9. Interferogram with highlighted fringe of constant velocity; taken at transonic regime (M_1 = 0.968), smooth leading edge

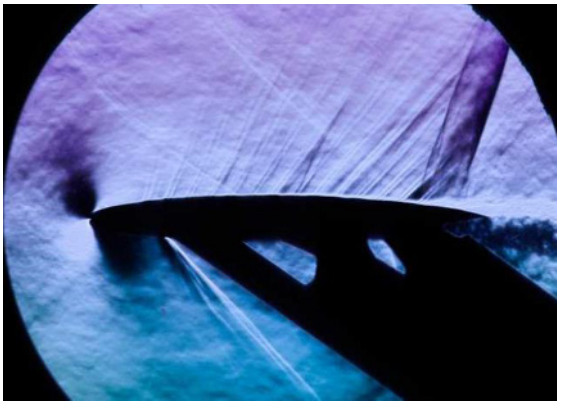

Fig. 10. Schlieren picture taken at M_1 = 0.988 showing flow disturbances on the upper surface of the airfoil due to imperfect coverage of leadwires

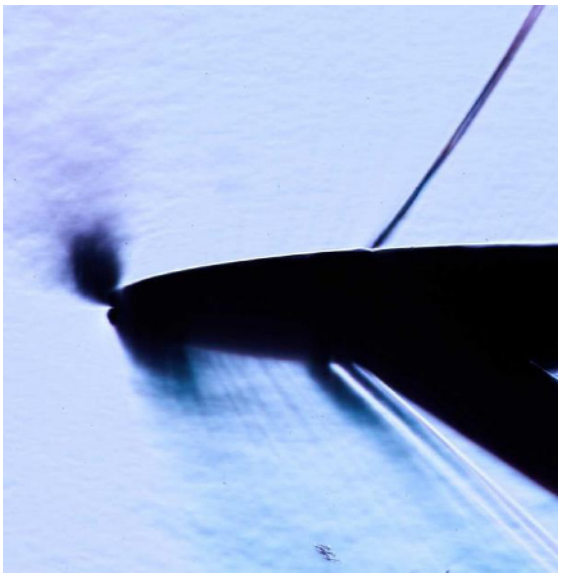

Fig. 11. Schlieren picture taken at M_1 = 0.989 showing origin of oblique shock eaves on backward facing steps due to rough tape (Ra~50)and the foil

4.3 Influence of rough tape

In the cases with rough leading edge, the rough tape with corundum grains which covers front 25% of the chord on both upper and lower surface forms backward facing step (Fig. 4). Height of this step depends on the applied roughness. Height of the step due to the rough tape is 0.21 mm in case of Ra~100 and (0.16÷0.19 mm) in case of Ra~50. Moreover, on the lower surface, this step adds to the step due to foil with hot-films (Fig. 4). Therefore, oblique shock originating at the step on the uppers surface is different from the shock originating at the step on the lower surface (Fig. 11). This increases flow asymmetry. On the other hand, the structure of the shock wave at the step provides information on the state of the boundary layer there. Thus, it partly compensates fact that the first 3 sensing elements of the hot-film array are covered with the tape.

5 Results

Graphs in Figures 12 and 13 show distributions of isentropic Mach number on the upper surface of the airfoil in subsonic and transonic case, respectively. Three curves in each graph correspond to cases with smooth and two variants of rough leading edge. Corresponding interferograms are provided in Figures 14 to 16.

In the case of subsonic flow, there are no substantial differences between distributions. Expansion at the leading edge up to 0.2c is somewhat less steep in the cases with rough leading edge, but there is no direct proportion between roughness and steepness of the expansion. Thus, it should be rather ascribed to somewhat changed shape of the leading edge due to the rough tape. Peaks at 0.22c in the cases with rough leading edge result from the flow over the backward facing step at the end of the rough tape. Differences between distributions at the rear part of the airfoil reflect different development of a thick boundary layer in cases with rough leading edge. Development of the boundary layer in subsonic cases is well documented by Schlieren pictures taken with the Toepler knife oriented parallel to the airfoil's axis of symmetry (Figures 17 and 18). In the case of rough leading edge (Fig. 18), the boundary layer at the trailing edge is twice as thick as in the case with smooth leading edge.

In the transonic case, the isentropic distributions of Mach number (Fig. 13) exhibit significant differences at the rear part of the airfoil. The thick boundary layer and its separation in the cases with rough leading edge change effective shape of the airfoil. This leads to an acceleration of the flow to higher Mach numbers and shifting of the normal terminating shock wave towards the trailing edge.

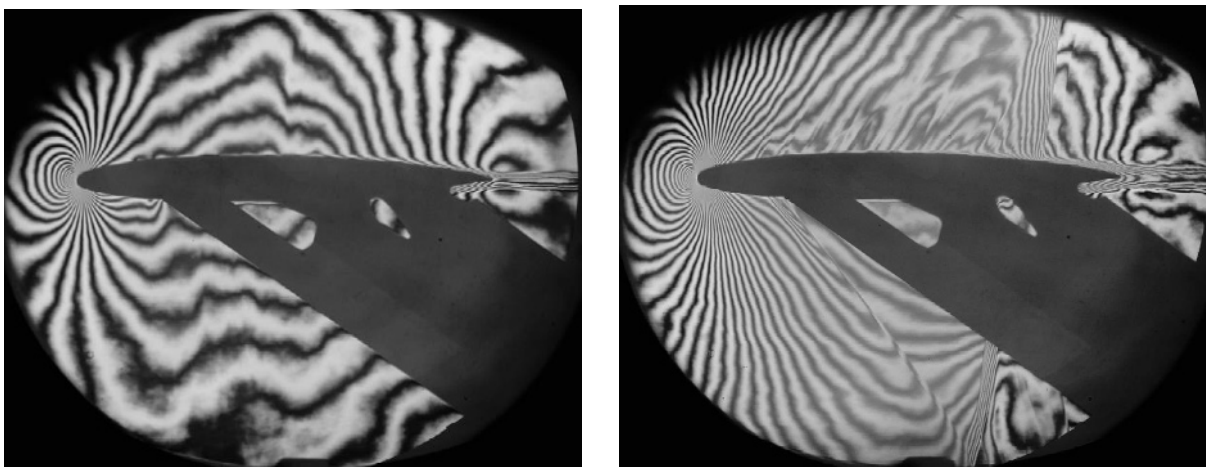

Fig. 14: Interferograms taken at subsonic case $M_1 = 0.75$ (left) and transonic case $M_1 = 0.97$ (right) - cases with smooth leading edge

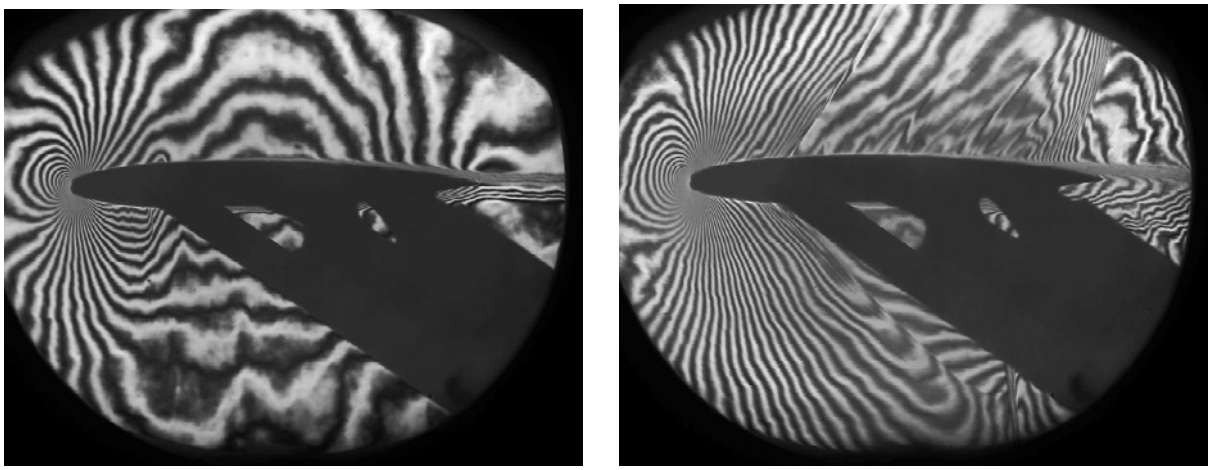

Fig. 15. Interferograms taken at subsonic case $M_1 = 0.75$ (left) and transonic case $M_1 = 0.97$ (right) - cases with rough leading edge (Ra~50)

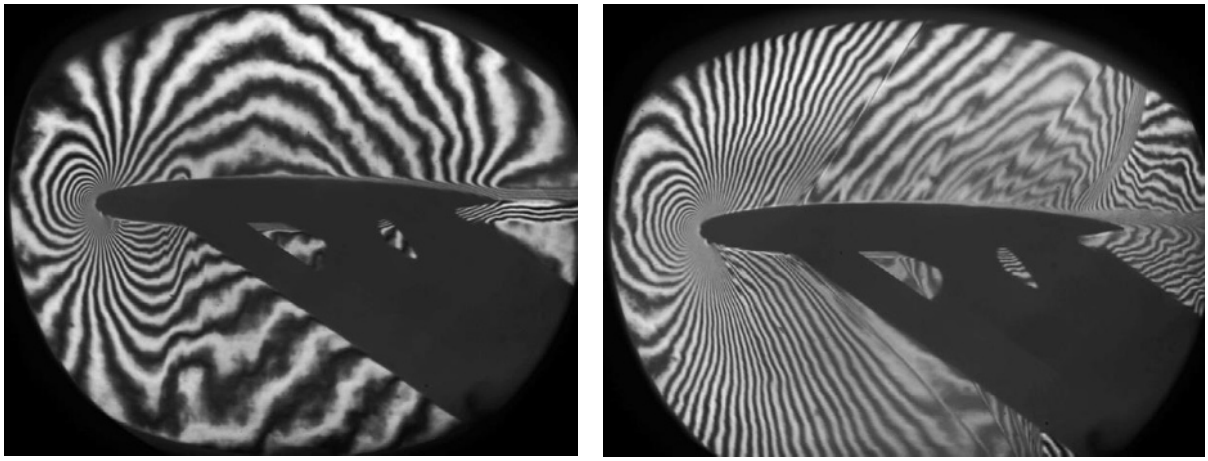

Fig. 16. Interferograms taken at subsonic case $M_1 = 0.75$ (left) and transonic case $M_1 = 0.97$ (right) - cases with rough leading edge (Ra~100)

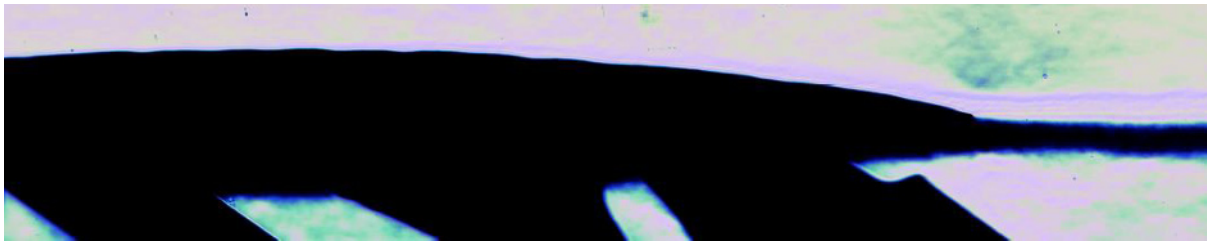

Fig. 17. Schlieren visualization of the upper surface boundary layer in case with smooth leading edge. ($M_1 = 0.76$)

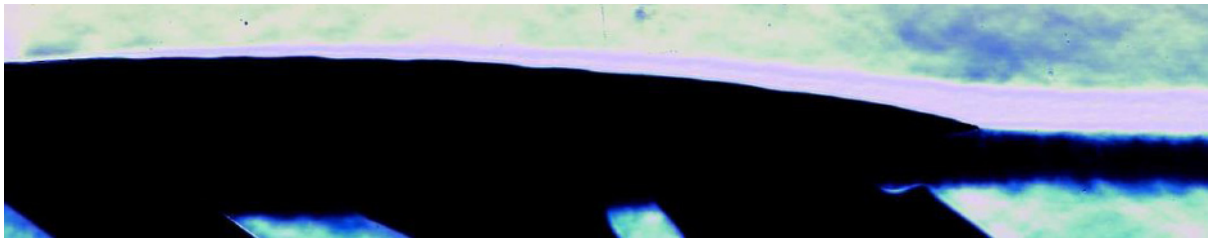

Fig. 18. Schlieren visualization of the upper surface boundary layer in case with rough leading edge. ($M_1 = 0.76$)

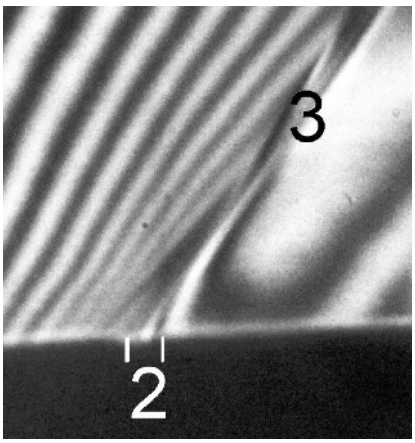

Fig. 19. Detail of an oblique shock wave origin on the airfoil's upper surface due to rough tape edge (rough leading edge)

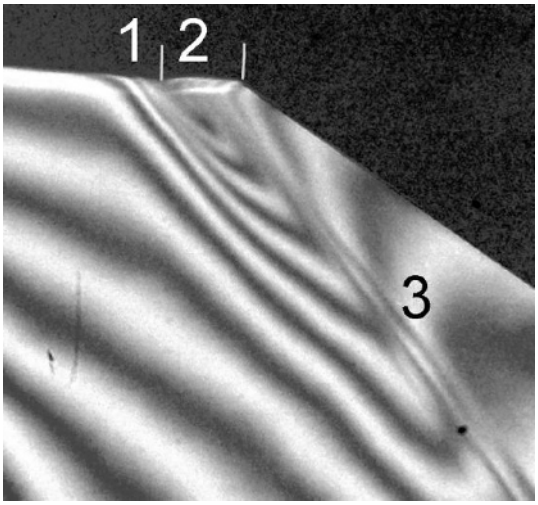

Fig. 20. Detail of an oblique shock wave origin on the airfoil's lower surface due to hot-film foil edge (smooth leading edge)

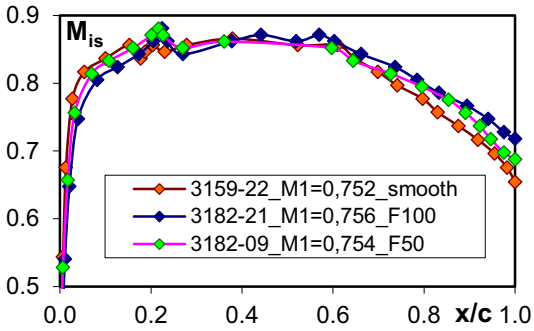

Fig. 21. Distribution of M_{is} along the profile at $M_1 = 0.75$ and various leading edge roughness

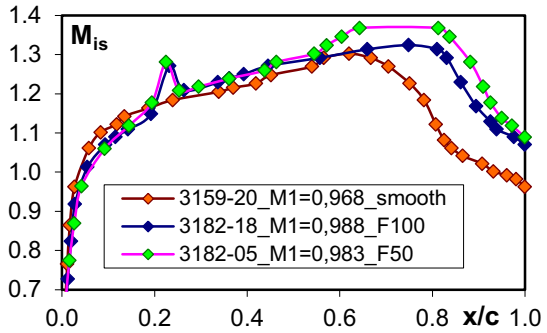

Fig. 22. Distribution of M_{is} along the profile at $M_1 = 0.98$ and various leading edge roughness

The oblique shock resulting from the flow past the backward facing step at the edge of the rough tape provides information on the state of the boundary layer there. Detail in Figure 19 show flow configuration at the origin of this shock wave. The rapid expansion at the edge of the rough tape is right away terminated by the shock wave. In contrast with this, Figure 20 shows flow configuration at the edge of the hot-film array foil on the airfoil's lower side. In this case the leading edge was smooth. It can be seen that the acceleration at the foil's edge (marked as 1 in Figure 20) is followed by relatively wide region of compression (marked as 2) before the shock wave (marked as 3). This indicates higher sensitivity of the boundary layer to interaction with the shock wave unlike in the previous case. It can be concluded from this that the boundary layer at the edge of the rough tape in Figure 19 is fully turbulent, whereas, in Figure 20 it is not.

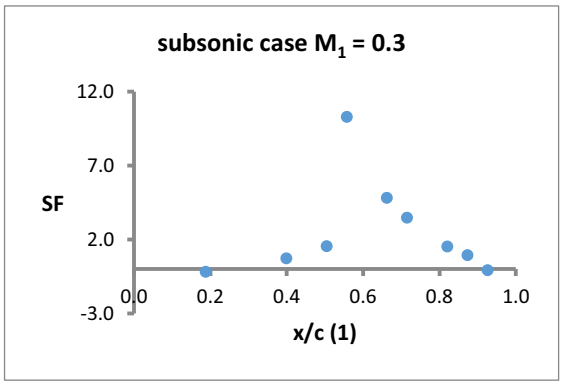

a) subsonic case $M_1 = 0.3$

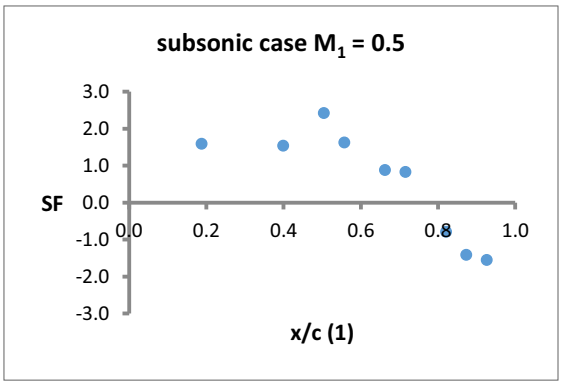

b) subsonic case $M_1 = 0.5$

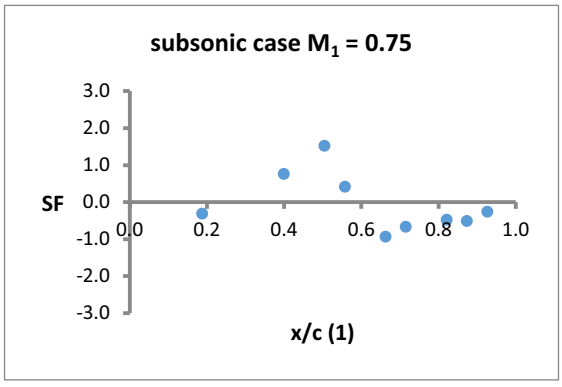

c) subsonic case $M_1 = 0.75$

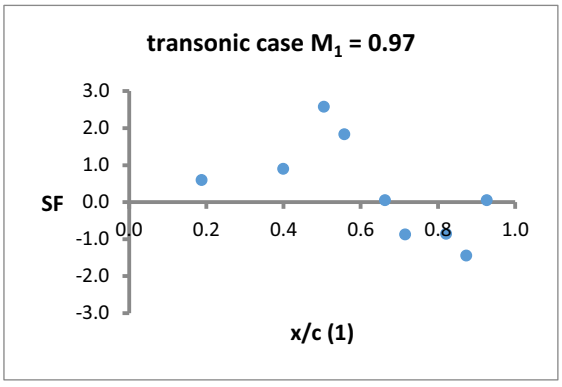

d) transonic case $M_1 = 0.97$

Fig. 23. Skew function SF along the upper blade surface for the case of the smooth blade for various inlet Mach numbers M_1.

Graphs in Figure 23 show the Skew Function along the blade upper surface for the case with the smooth surface and for various inlet Mach numbers M_1. As described by Hodson [3] and Tiedemann [4], it might be possible to estimate both the location of the transition onset and its end based on the Skew Function distribution. In both cases (rough and smooth blade), the transition occurred in the attached flow. In the case of smooth surface, the transition onset shifts towards the leading edge with increasing inlet Mach number which is in accordance with available data obtained for similar airfoils [1]. For the inlet Mach number $M_1 = 0.3$, the transition onset is at the location $x/c \approx 0.4$ while for $M_1 = 0.75$ it shifts to $x/c \approx 0.25$. At the same time, the length of the transition region shortens and the whole regions shifts upstream.

Graphs in Figure 24 show the distribution of the Skew Function along the blade upper surface for the cases with the roughened leading edge and for various inlet Mach numbers M_1. Unlike in the case of smooth surface, the whole transition occurs at the roughened leading edge for both roughness values and all inlet Mach numbers. Hence, the transition significantly shifts upstream and the transition length is shortened. Therefore, it is likely that in the transonic cases, the possible shock wave – boundary layer interaction takes place in the turbulent boundary layer without the flow separation. Results obtained using the hot film array seems to be in good agreement with the results of the optical investigation.

6 Conclusions

Despite a number of shortcomings, current measurements proved usability of hot-films as a mean of boundary layer transition investigation in high subsonic and transonic flows past an airfoil. Results obtained by the hot-films are in good agreement with flow features observed in flow field images taken by interferometry and Schlieren technique.

Nomenclature

m	number of samples
SF	skewness function
$\bar{V}_b$	signal mean value
v'_b	deviation from the mean value

.

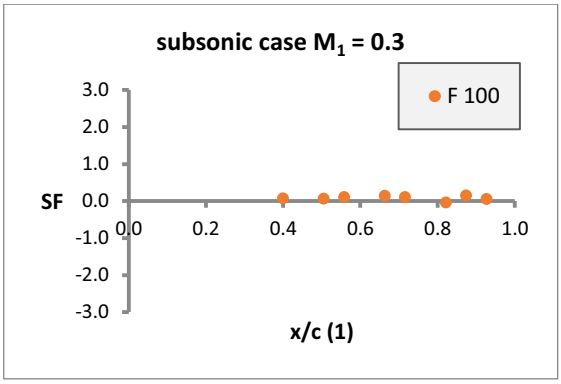

a) subsonic case $M_1 = 0.3$

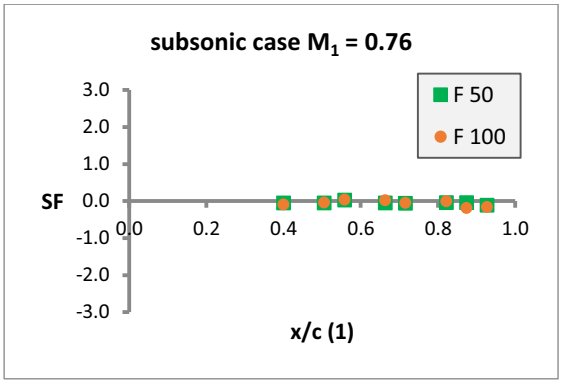

b) subsonic case $M_1 = 0.75$

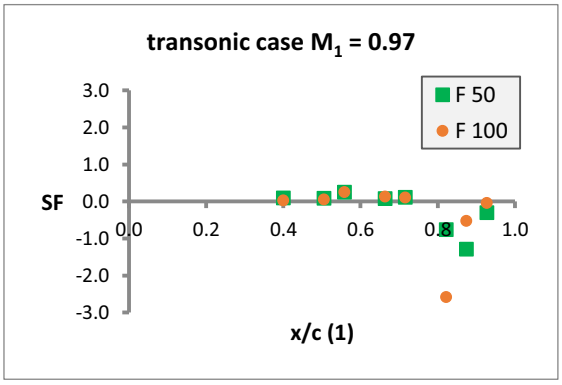

c) transonic case $M_1 = 0.97$

Fig. 24. Skew function SF along the blade upper surface for the case of the roughened leading edge of the blade for various inlet Mach numbers M_1 and roughnesses Ra~50µm (F 50) and Ra~100µm (F 100)

Acknowledgements

The authors would like to express their thanks to the Technology Agency of the Czech Republic which supported this research under the grant no. TH02020057. Institutional support RVO: 61388998 of the Institute of Thermomechanics of the Czech Academy of Sciences is also gratefully acknowledge

References

1. A. Bertelrud, *Transition on a Three-Element High Lift Configuration at High Reynolds Numbers*, AIAA Paper 98-0703 (1998) https://doi.org/10.2514/6.1998-703
2. M. Luxa, J. Příhoda, D. Šimurda, P. Straka , J. Synáč, J. Therm. Sci., **25**(2): 138-144 (2006)
3. H. P. Hodson, I. Huntsman, A. B. Steele, J. Turbomach., **116**(3): 375-383 (1993)
4. M. Tiedemann, F. Kost, *Unsteady Boundary Layer Transition on a High Pressure Turbine Rotor Blade*, ASME Paper 99-GT-194 (1999)
5. A. Aharoni, *How to Adjust the Frequency Response of a CT Anemometer*. A. A. Lab Systems, Ramat-Gan, Israel. Available from: https://www.lab-systems.com/products/flow-mea/Adjusting%20the%20frequency%20response/How%20to%20set%20the%20frequency%20response%20of%20a%20CT%20anemometer.pdf